12-1-2023

MAPK1 promotes the metastasis and invasion of gastric cancer as a bidirectional transcription factor

Yue Wang

Zheng Guo
Edith Cowan University

Yueli Tian

Liang Cong

Yulu Zheng
Edith Cowan University

See next page for additional authors

Authors

Yue Wang, Zheng Guo, Yueli Tian, Liang Cong, Yulu Zheng, Zhiyuan Wu, Guangle Shan, Yao Xia, Yahong Zhu, Xingang Li, and Ying Song

MAPK1 promotes the metastasis and invasion of gastric cancer as a bidirectional transcription factor

Yue Wang[1], Zheng Guo[2], Yueli Tian[1], Liang Cong[1], Yulu Zheng[2], Zhiyuan Wu[2], Guangle Shan[3], Yao Xia[4,5], Yahong Zhu[3], Xingang Li[2*] and Ying Song[1*]

Abstract

Background The Mitogen-activated protein kinase 1 (MAPK1) has both independent functions of phosphorylating histones as a kinase and directly binding the promoter regions of genes to regulate gene expression as a transcription factor. Previous studies have identified elevated expression of MAPK1 in human gastric cancer, which is associated with its role as a kinase, facilitating the migration and invasion of gastric cancer cells. However, how MAPK1 binds to its target genes as a transcription factor and whether it modulates related gene expressions in gastric cancer remains unclear.

Results Here, we integrated biochemical assays (protein interactions and chromatin immunoprecipitation (ChIP)), cellular analysis assays (cell proliferation and migration), RNA sequencing, ChIP sequencing, and clinical analysis to investigate the potential genomic recognition patterns of MAPK1 in a human gastric adenocarcinoma cell-line (AGS) and to uncover its regulatory effect on gastric cancer progression. We confirmed that MAPK1 promotes AGS cells invasion and migration by regulating the target genes in different directions, up-regulating seven target genes (*KRT13*, *KRT6A*, *KRT81*, *MYH15*, *STARD4*, *SYTL4*, and *TMEM267*) and down-regulating one gene (*FGG*). Among them, five genes (*FGG*, *MYH15*, *STARD4*, *SYTL4*, and *TMEM267*) were first associated with cancer procession, while the other three (*KRT81*, *KRT6A*, and *KRT13*) have previously been confirmed to be related to cancer metastasis and migration.

Conclusion Our data showed that MAPK1 can bind to the promoter regions of these target genes to control their transcription as a bidirectional transcription factor, promoting AGS cell motility and invasion. Our research has expanded the understanding of the regulatory roles of MAPK1, enriched our knowledge of transcription factors, and provided novel candidates for cancer therapeutics.

Keywords Gastric cancer, MAPK1, Bidirectional transcription factor, Cancer progression

*Correspondence:
Xingang Li
xingang.li@ecu.edu.au
Ying Song
songying@jlu.edu.cn
[1]Gastroenteric Medicine and Digestive Endoscopy Center, The Second
Hospital of Jilin University, Changchun, Jilin, China

[2]Centre for Precision Health, Edith Cowan University, Joondalup, WA,
Australia
[3]Department of Bioinformatics, Thrive Bioresearch, Beijing, China
[4]School of Science, Edith Cowan University, Joondalup, WA, Australia
[5]Department of Microbiology, School of Clinical Medicine, Li Ka Shing
Faculty of Medicine, The University of Hong Kong, Pokfulam, Hong Kong
Special Administrative Region, China

Wang *et al. BMC Cancer*   (2023) 23:959

Page 2 of 13

Background

Gastric cancer ranks among the top five most common cancers and is the third leading cause of cancer-related deaths worldwide, accounting for an estimated 1 million new cases and 723,000 deaths each year annually [1]. The incidence of gastric cancer (GC) exhibits notable variations concerning sex and geographical distribution. The high incidence incidence and mortality hotspots for GC are particularly prevalent in East Asia, encompassing regions such as China and Japan, as well as in Central and South America, and Eastern Europe [2]. It is noteworthy that the susceptibility to GC is approximately twice as high in males as it is in females [3]. Numerous well-established risk factors have been associated with the development of GC, including but not limited to family history, diet habits, alcohol consumption, smoking, and infections with Helicobacter pylori and Epstein-Barr virus [2].

The classification of GC has witnessed the formulation of several systems due to diverse morphological manifestations. Notable examples include the classifications proposed by Nakamura and colleagues [4], Lauren [5], and WHO [6]. The Lauren classification holds prominence as the most commonly utilised system, while the WHO classification is hailed for its comprehensive and intricate categorisation of GC subtypes. In clinical practice, the lack of noticeable symptoms in the early stages of gastric cancer, and the fact that this disease is often mistaken for other conditions, coupled with this cancer's characteristic to invade surrounding tissues and metastasize to distal organs, results in that gastric cancer is often diagnosed at an advanced stage [7].

Due to these well-documented epidemiological and classification factors, gastric cancer continues to exhibit a substantial mortality rate, reaching as high as 75% in various regions across the globe. This sobering statistic underscores the pressing need for further research and clinical interventions to effectively address this formidable health challenge [8]. While chemotherapy is a standard treatment for advanced gastric cancer, the median overall survival with standard chemotherapy often remains around eight months [9]. Achieving effective chemical treatment of gastric cancer relies on the inhibition of invasion and metastasis, emphasizing the importance of exploring underlying molecular processes and identifying master modulators for the development of novel targeted medications [10].

Mitogen-Activated Protein Kinase 1 (MAPK1) is an extensively studied member of the MAP kinase family, also known as extracellular signal-regulated kinases 2 (ERK2) [11, 12]. Being an essential member, MAPK1 functions in several cell signalling cascades mediating diverse cellular processes, including immune responses, proliferation, differentiation, and development [13–15]. Under normal physiological conditions, MAPK1 expression is modest and persistent in most tissues, but it undergoes significant changes in several malignancies including breast, bladder, lung, and gastric cancers [16].

Traditional in vitro tests mainly identified the role of MAPK1 in gastric cancer processes as a protein kinase. Overexpression of the *MAPK1* gene has been associated with cell migration in BGC-823 gastric cancer cells [17], while downregulation of the *MAPK1* gene significantly decreases the proliferation of MGC-803 gastric cancer cells, leading to cell cycle progression, and promote apoptosis [18]. However, MAPK1 has also been characterised as a transcription factor (TF), capable of binding to a G/CAAAG/C consensus sequence at the promoter and repressing the expression of interferon gamma-induced genes [19]. This raises the question of whether MAPK1 functions in the invasion and malignancy of gastric cancer by acting as a transcription regulator.

Transcirption factors (TFs) control chromatin and transcription by attaching to specific DNA sequences, thereby regulating gene expression and constructing to cancer development [20, 21]. Decades of research have proven that TFs with abnormal expression or functional defects can lead to uncontrolled cell proliferation and cancer development [22]. While earlier investigations into transcriptional regulation in cancer focused on TFs as transcriptional activators, recent studies have unveiled multiple alternative mechanisms of transcriptional repression in cancer. These mechanisms present potential therapeutic targets for the development of targeted anti-cancer agents [23]. Given MAPK1's dual characteristics as both a MAP kinase and a transcription repressor, we focused on whether MAPK1 function as a transcription factor in the processes of invasion and metastasis in gastric cancer.

In our current study, we employed integrated approaches, including gene overexpression, gene knockdown, RNA sequencing (RNA-seq), and ChIP sequencing (ChIP-seq), to investigate the transcription regulatory function of MAPK1 and its effect on the procession of gastric cancer.

Methods

Cloning and over-expression plasmid construction

The plasmid for stable overexpression of MAPK1 was achieved by inserting the full-length coding sequence (CDS) of MAPK1 into a proper plasmid. Briefly, the MAPK1 CDS was obtained by reverse transcription-polymerase chain reaction (RT-PCR) using the complementary DNA (cDNA) of AGS cells as a template. The primers for RT-PCR were designed in terms of the gene annotation of GRCh38.p13 human genome assembly in the Ensembl database (https://asia.ensembl.org/Homo_sapiens/Info/Index). Then, the CDS was cloned into

pOE3.1-CAHyg plasmid (JTS Scientific, Wuhan, China) for later experiments.

AGS cell culture and over-expression plasmid transfection

Human gastric adenocarcinoma epithelial cell line (AGS cells, CRL-1739) from American Type Culture Collection (ATCC, Rockville, MD, USA) were cultured in Dulbecco's Modified Eagle Medium: Nutrient Mixture F12 medium (DMEM/F12) (Gibco, GrandIsland, NY, USA) with 10% fetal bovine serum, 100 g/mL streptomycin, and 100 U/mL penicillin at 37 °C and 5% CO_2.

Using Lipofectamine 2000 (Invitrogen, Carlsbad, CA, USA), all cell transfection was carried out following the manufacturer's instructions. We used an empty pOE3.1-CAHyg plasmid vector as a non-targeting control to examine if the transfection reagents or the transfection process itself had any cytotoxic effects on target cells, i.e., ACS cells.

For a quantitative real-time polymerase chain reaction (qRT-PCR) investigation, the total RNA of transfected cells was extracted with TRIzol reagent (Thermo Fisher Scientific, Waltham, MA, USA) 48 h after transfection.

Assessment of gene expression of MAPK1 by qPCR

Glyceraldehyde-3-phosphate dehydrogenase gene (*GAPDH*) was used as the control gene to assess the effects of oe-*MAPK1*. Standard protocols were used for cDNA synthesis as prescribed in previous studies [24]. Briefly, a cDNA core kit (Promega, Madison, WI, USA) was used to generate complementary DNA from 500ng of total RNA. Quantitative RT-PCR was carried out on a Bio-Rad S1000 using Hieff™ qPCR SYBR® Green Master Mix (Low Rox Plus; YEASEN, China). Table S1 displays the primer sequences. The $2^{-\Delta\Delta CT}$ approach was then used to normalize the transcript concentrations to the *GAPDH* mRNA level [25].

Both over-expressed MAPK1 AGS cells and MAPK1 knockdown AGS cells were tested by this method for the assessment of MAPK1 gene expression.

Assessment of protein expression of MAPK1 by western blot analysis

Extraction of total proteins from oe-MAPK1 AGS cells was performed using a lysis buffer (Beyotime, Shanghai, China), and the amount of protein recovered was determined with a bicinchoninic acid protein assay kit (Beyotime, Shanghai, China).

The proteins were transferred from the polyvinylidene difluoride (PVDF) membrane to a PVDF plate using sodium dodecyl sulphate polyacrylamide gel electrophoresis (SDS-PAGE) (Millipore, Bedford, MA, USA). Subsequently, the blots were cut based on the marker position prior to hybridization with antibodies during blotting, allowing the isolation of specific bands representing MAPK1 and Lamin A/C. After being rinsed in tris-buffered saline with 0.1% tween 20 detergent, the membrane was blocked for 1 h with skim milk powder (5%) before being incubated overnight with primary antibodies, i.e., anti-MAPK1 anti-GAPDH or anti-Lamin A/C (Thermo Fisher Scientific, Waltham, MA, USA) at 4 °C.

Anti-GAPDH or anti-Lamin A/C was used as the loading control antibody for this Western Blot to normalize the levels of MAPK1 protein detected by confirming that protein loading was the same across the SDS-PAGE gel.

The membrane was washed and subjected to incubation with goat anti-rabbit immunoglobulin (Ig) G secondary antibody for 1 h at room temperature, and then signals were detected using automated Tanon 4600SF chemiluminescence imaging equipment (Tanon Science & Technology, Shanghai, China).

Similar to the assessment for gene expressions, the protein expressions in both over-expressed and knockdown MAPK1 AGS cells were tested by this method.

Transwell migration assay and invasion assay

To examine the effects of oe-MAPK1 on the migration and invasion of AGS cells establishes oe-MAPK1 cells were counted and seeded in the upper compartment of the Transwell migration and invasion chambers (Thermo Fisher Scientific, Waltham, MA, USA), respectively. The complete medium was introduced into the lower chamber in both tests. Cells from the top layer were wiped off using a cotton swab after 24 h in 5% CO_2 at 37 °C. While the bottom chamber cells were randomly counted in three different microscope fields after being fixed with paraformaldehyde (4%), dyed with crystal violet (0.1%), and examined under a microscope.

In the invasion and migration experiments, Control, NC, and oe-MAPK1 groups were each repeated three times. The Transwell chamber with 100 µl Matrigel was used for the invasion test. All other processes were the same as for the Transwell migration assay.

Knockdown of MAPK1 in AGS cells by siRNA

The sequences for siRNA against MAPK1 were designed using *siRNA at Whitehead* [26], a web-based tool developed by the Whitehead Institute for Biomedical Research (http://sirna.wi.mit.edu/). The sequences of siRNA and non-targeting control siRNA (siNegative RNA) were listed in Supplementary Table S1. All siRNA duplexes were purchased from Gemma (Suzhou, China).

Library construction for RNA-seq

The RNA-seq libraries were created according to the manufacturer's guidelines. Briefly, the whole RNA was processed with RQ1 DNase (Promega, Madison, WI, USA) to eliminate DNA contamination. Using Smart-Spec Plus (Bio-Rad, Hercules, CA, USA), we measured

the RNA's absorbance at 260 and 280 nm (A260/A280) to evaluate its purity and concentration. Another method utilized the 1.5% agarose gel electrophoresis to confirm RNA purity.

NEBNext® UltraTM Directional RNA Library Prep Kit for Illumina® (New England Biolabs, Ipswich, MA, USA) was used to prepare RNA-seq libraries from 1 μg of total RNA from each sample. Double-strand cDNA was synthesized by purifying and fragmenting polyadenylated mRNAs. The DNAs were ligated to diluted NEBNext® Adaptor after end repair and "A" tailing. Single-strand cDNA was amplified, purified, quantified, and kept at -80 °C before sequencing; this was accomplished by first digesting the purified ligation products corresponding to 300–500 base-pairs (bp) with heat-labile uracil-DNA glycosylase (New England Biolabs, Ipswich, MA, USA).

After the quality control for libraries, NovaSeq 6000 system (Illumina, San Diego, CA, USA) was used to sequence in a mode of 150 nt paired-end reads.

RNA-seq raw data clean and alignment
First, raw data longer than 2-N bases were thrown out. Raw sequencing reads were cleaned of adaptors and low-quality bases using the FASTX-Toolkit (Version 0.0.13). The study also eliminated the short reads containing less than 16 nt. Bowtie2 [27], was used to align the clean reads to the GRCh38 genome, with a maximum of four mismatches. For the purposes of counting gene reads and calculating FPKM (fragments per kilobase of transcript per million fragments mapped), only uniquely mapped reads were used [28].

Differentially expressed gene analysis
In order to identify differentially expressed genes (DEGs), the *edgeR* package version 3.18.1 (R Bioconductor package) was employed [29]. The criterion for determining DEGs was established at a P-value for correction of <0.05 and a fold change of >1.5 or <0.67, respectively.

Chromatin immunoprecipitation sequencing for MAPK1
After 10 min of incubation at room temperature, AGS cells were cross-linked with formaldehyde (final concentration of 1%). Glycine was added to a final concentration of 0.125 M and gently mixed to halt the cross-linking reaction. On the ice, cells that had been cross-linked with formaldehyde were lysed by resuspending 10 cell pellet volumes of RIPA buffer (50 mM Tris 7.4, 150 mM NaCl, 2 mM EDTA, 0.1% SDS, 0.5% NP-40, and 0.5% deoxycholate) and pipetting them repeatedly.

Sonication of cell lysates resulted in DNA fragments of 200–500 bp being centrifuged at 12,000 g for 10 min, and the supernatant was used for immunoprecipitation without further processing.

After placing the tube containing the Pierce™ ChIP-grade Protein A/G Magnetic Bead (Thermo Fisher Scientific, Waltham, MA, USA) on the magnetic stand, the supernatant was discarded. Utilizing sodium phosphate buffer (1 mL, 0.1 M), the beads were washed thrice. 200 μL of 0.1 M sodium phosphate buffer was used to resuspend the beads. To the tube containing the beads was added 10 μg of MAPK-antibody (Cell Signaling Technologies, Danvers, MA, USA, #9102s) and normal IgG (Cell Signaling Technologies, Danvers, MA, USA, #2729s) antibody. The substance was put in a revolving wheel and kept there for 2 h at 4℃. The magnetic stand was turned on for 1 min with the tube holding the beads inside, and then the supernatant was poured out. Beads were resuspended with cell lysates. After being overnight spun at 4 °C, the sample was transferred to the magnetic stand and the supernatant was discarded. After being soaked in TE buffer (10 mM Tris [pH 8.0], 1 mM EDTA [pH 8.0]), the beads were washed five times with LiCl IP Wash Buffer (100 mM Tris [pH 7.5], 500 mM LiCl, 1% NP-40, and 0.5% deoxycholate).

The material was lyophilized, resuspended in 100 μL of Elution Buffer (100 mM NaHCO3, 1% SDS), and reverse cross-linked by incubation at 65 °C for a whole night. Purified DNA fragments were obtained using phenol extraction and ethanol precipitation after being treated with RNase A and proteinase K sequentially. 10 μL of water was used to resuspend the DNA pellet.

Following the manufacturer's instructions, short, purified DNA fragments were end-repaired, adenylated, ligated to adaptors, and PCR amplified to create libraries using the KAPA HTP Library Preparation Kit (KAPA Biosystems, Wilmington, MA, USA, #KK8234). The libraries were created following the manufacturer's instructions and used with the NovaSeq 6000 system (Illumina, San Diego, CA, USA) for 150 nt paired-end sequencing in high-throughput sequencing.

ChIP-seq data analysis
Only reads that were uniquely mapped to the human GRCh38 genome after being aligned with Bowtie2 [27], were used for the following analysis. We utilized model-based analysis for ChIP-seq version 1.4 to find the binding locations of MAPK1 [30]. The background noise was assumed to be the input samples that did not undergo immunoprecipitation which was filtered by a linear signal-noise model in a previous study [31]. The peaks' locations in relation to the transcription start site (TSS) were assigned using *DeepTools* [32], and binding profiles were visualized using this program.

To find the enriched binding motifs in peaks, we employed the Hypergeometric Optimization of Motif EnRichment (HOMER) program [33]. For visualizing the genome hits of RNA-seq and ChIP-seq, sashimi plots

were created using the Integrative Genomics Viewer (IGV) (https://software.broadinstitute.org/software/igv/home) [34].

Functional enrichment analysis

We used the KOBAS 2.0 server [35] to identify Gene Ontology (GO) terms and Kyoto Encyclopedia of Genes and Genomes (KEGG) pathways to classify DEGs and peak-associated genes according to their biological function [36]. A controlling approach based on the Benjamini-Hochberg method for the false discovery rate (FDR) statistic and the hypergeometric test were employed to determine the degree to which each term was enriched.

Clinical data analysis

We obtained gene expression and clinical data of gastric cancer from the TCGA database (https://portal.gdc.cancer.gov) and extracted the outcome events, survival time, and target gene expression values [37]. Then we assigned gastric cancer samples to two groups (high and low expression groups), with the median of the target genes' expression value as the cutoff value. Kaplan-Meier survival analysis and log-rank test were performed using packages (*survival 3.3.1*, *survminer*, *ggplot2 3.3.6*) in R software, version 4.1.0 (R Foundation, Austria).

Statistical analysis

Each experiment was conducted in triplicate to estimate the mean±standard deviation (SD). GraphPad Prism software version 8 (GraphPad PRISM, La Jolla, CA, USA) was used for the statistical analysis. To quantify the differences between the two groups, we employed the paired Student's t-test when the homogeneity of variance assumption was satisfied between groups; otherwise, the Wilcoxon-signed rank test was used. $p < 0.05$ was set to indicate minimum statistical significance.

Results

Effect of overexpressed MAPK1 in AGS cells

To investigate the role of MAPK1 in the development of gastric cancer, we transfected AGS cells, a common human gastric cancer cell line, using the overexpression plasmid of MAPK1 (oe-MAPK1). We conducted qRT-PCR and Western blotting analysis to examine the mRNA and protein levels, respectively.

In AGS cells transfected by oe-MAPK1 plasmids, results from both qRT-PCR and Western blotting analysis demonstrated a dramatically increased MAPK1 expression in case (oe-MAPK1) cells compared to control cells ($P < 0.001$) (Fig. 1A, B). There were no significant differences between control and non-targeting control cells, which ensured the transfection reagents, and the transfection process were non-cytotoxic to AGS cells.

Then, the function of oe-MAPK1 in cell invasion and migration was determined using transwell experiments. Oe-MAPK1 cells showed significantly induced cell proliferation and colony formation compared to control cells or non-targeting control cells. MAPK1 overexpression was shown to greatly increase the AGS cell migration ($P < 0.001$) and invasion ($P < 0.05$) (Fig. 1C, D). The non-significant differences between oe-MAPK1 cells and non-targeting control cells ensured the reliability of the experimental results.

Transcriptome profiling of gene expression alteration in short interfering-MAPK1 AGS cells

To inspect the regulatory effect of MAPK1 in gastric cancer, we next designed three short interfering RNAs (siRNAs) (Table S1) for *MAPK1* knockdown in AGS cells followed by RNA-seq for transcriptome profiling.

Three replicates of AGS cells were used for both siRNAs and non-targeting control (NC) AGS cells to generate a *MAPK1*-knockdown AGS cell model. The impact of MAPK1 regulation on gene expression was also analysed by RNA-seq. The qRT-PCR results showed that all three siRNAs significantly reduced mRNA levels of *MAPK1* (Fig. 2A) (qRT-PCT primer sequences in Table S2), indicating that the three siRNAs we designed can successfully knock down *MAPK1* in AGS cells. The siRNA1-knockdown AGS cells were then randomly chosen for subsequent experiments.

In further RNA-seq analysis, the *MAPK1* expression level in the FPKM (fragments per kilobase million) value showed a statistically significant decrease in the si-MAPK1 AGS cells compared to the NC AGS cells (Fig. 2A) (quality control results of RNA-seq in Table S3). FPKM-based principal component analysis (PCA) of all expressed genes indicated that the si-MAPK1 group and the NC group were well-separated (Fig. 2B), suggesting that the two groups could be differentiated from each other.

Through the use of the thresholds *P*-value for correction<0.05 and fold change>1.5 or <0.67, *edgeR* was able to identify a total of 111 differentially expressed genes (DEGs) (Table S4, Fig. 2C), comprising 31 upregulated genes and 80 downregulated genes. The MAPK1-mediated transcription was very consistent across three independent replicates, as shown by a hierarchical clustering heat map based on all DEG expression levels (Fig. 2D). The *MAPK1* knockdown treatment drastically altered the expression of a subset of genes, as shown by these findings.

GO and KEGG enrichment analyses were conducted using these DEGs to enrich their probable biological roles. We discovered that the GO enrichment findings of downregulated genes were mostly enriched in positive regulation of gene expression, cytokine-mediated
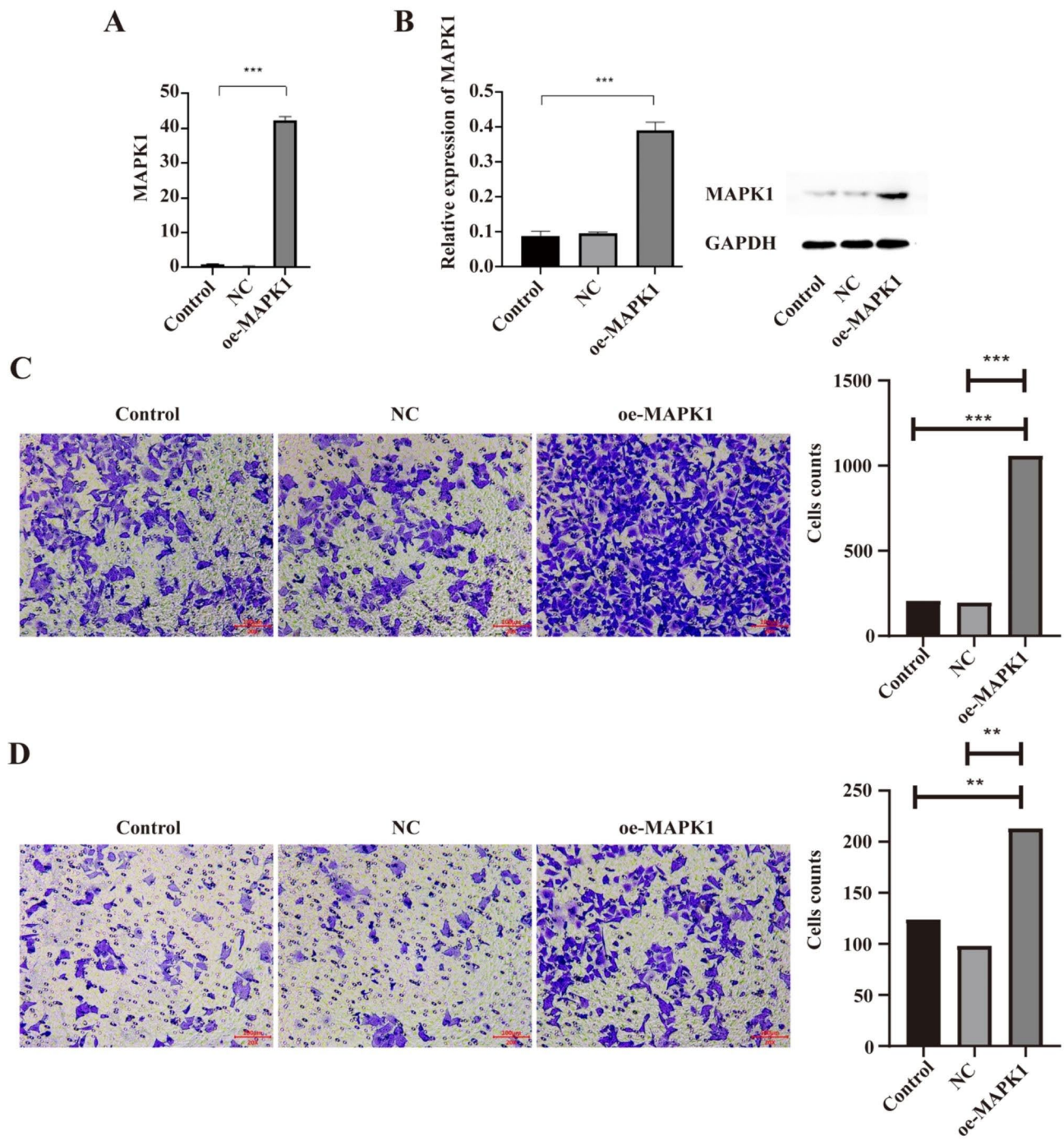
Wang *et al. BMC Cancer*   (2023) 23:959

Page 6 of 13

Fig. 1 Overexpression of MAPK1 promotes migration and invasion of AGS cells. (**A**) qRT-PCR detected that significantly increased MAPK1 mRNA expression in oe-MAPK1 AGS cells compared to control cells. (**B**) Western blot analysis showed increased expression of MAPK1 in oe-MAPK1 cells compared with control cells. (**C**, **D**) In Transwell assays (20 ×), migration and invasion were increased in oe-MAPK1 AGS cells. Cells were counted in five randomly selected fields and data are presented as the means ± SEM and were evaluated using Student's t-test (n = 3). Error bars show the mean ± SEM. **P < 0.01 and ***P < 0.001. NC: non-targeting control; oe-MAPK1: overexpression of MAPK1; SEM: standard error of the mean

signalling pathway, apoptotic process, and positive regulation of cell population growth (Fig. 2E). Among the detected DEGs, we found 10 representative down-regulated genes that were previously reported to be involved in cell proliferation and migration, i.e., *CCND1*, *CXCL8*, *EMP3*, *ITGA2*, *KRT6A*, *KRT13*, *KRT17*, *KRT81*, *MAL2*, and *PADI1* (Fig. 2F). These positive associations between gene expressions of MAPK1 and DEGs indicate that these genes are likely the risk factors for the migration and invasion of AGS cells. On the contrary, the
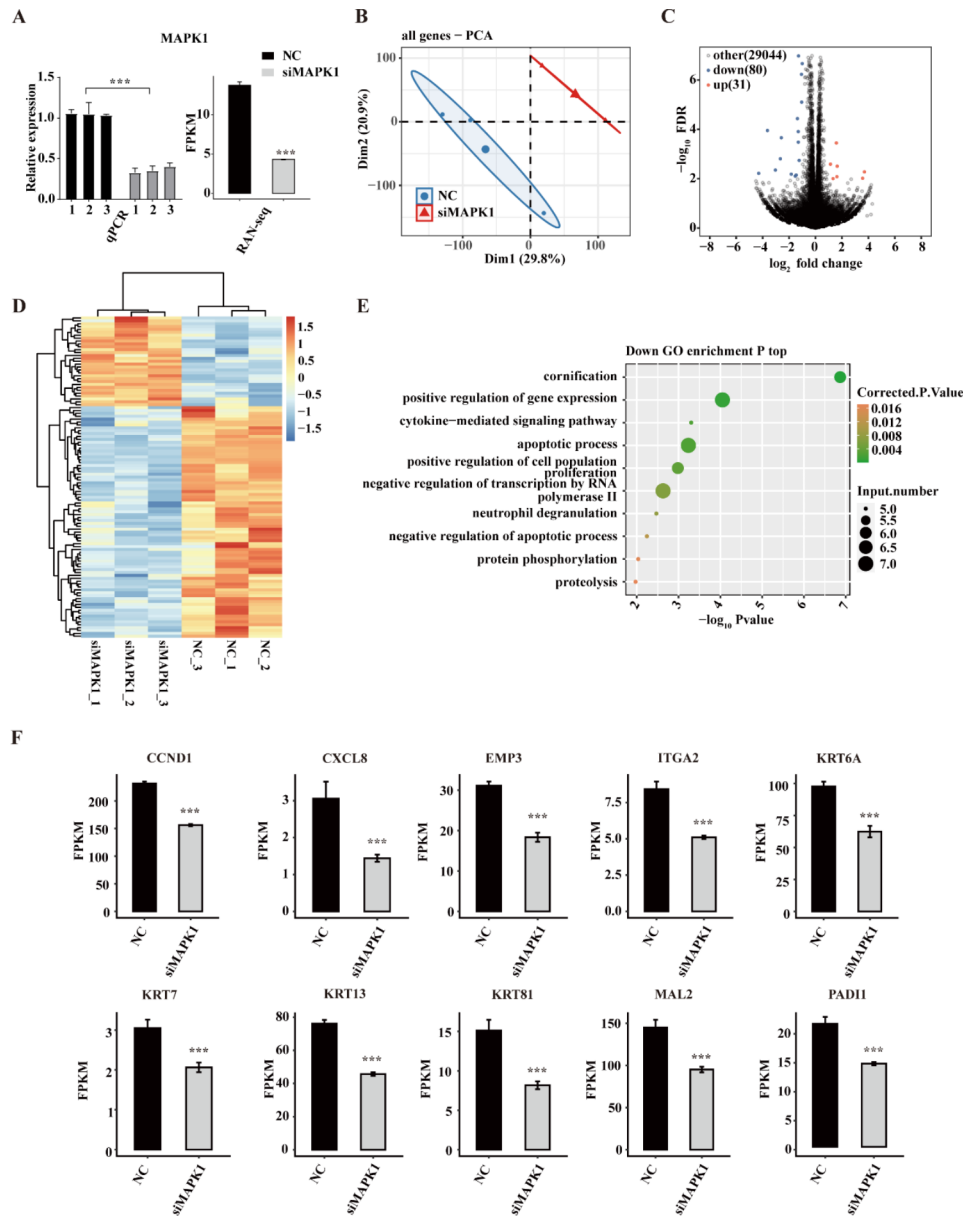
Fig. 2 Transcriptome profiling of gene expression alteration in si-MAPK1 AGS cells. (**A**) Validation of interference effect. The effectiveness of the interference of miRNA was assessed using qRT-PCR and RNA-seq. (**B**) PCA using the FPKM value of every gene MAPK1 knockdown that was found. The confidence ellipse is the ellipse for each group. (**C**) A volcano plot displaying all DEGs that vary in expression between knockdown and NC samples. (**D**) A heat map was created using hierarchical clustering that displays the expression levels of each DEG. (**E**) Scatter plot displaying the downregulated DEGs' enhanced GO biological process data. (**F**) A bar graph displaying the DEGs' statistical differences and the pattern of several key genes' expressions. Error bars show the mean ± SEM. ***P < 0.001. SEM: standard error of the mean

significantly upregulated DEGs in knockdown MAPK1 AGS cells whose expressions are negatively associated with MAPK1, are potential protective factors.

MAPK1 extensively interacts with genes by binding to their regulatory regions

To obtain MAPK1 binding characteristics on chromatin, we profiled the MAPK1-binding genes at the genome-wide level by ChIP-seq approach.

We used MAPK1 and IgG antibodies to immuno-precipitate (IP) proteins from the lysate of AGS cells and subsequently detected them using Western Blotting analysis. Based on the data, it was determined that the MAPK1 antibody had a high degree of specificity, and MAPK1-binding DNA fragments could be effectively separated from unbound oligonucleotides (Fig. 3A). We prepared two replicates for both IP samples (IP1 and IP2) and corresponding background noises (Input1 and Input2) which were assumed not to undergo

Wang *et al. BMC Cancer*   (2023) 23:959

Page 8 of 13

immunoprecipitation, respectively. The quality control of sequencing reads was conducted using FastQC [38], and the quality met the requirements for consequent analysis (Table S5).

Compared to the corresponding background noise (input sample), the IP sample had a considerably larger number of enriched genes, as shown by a correlation analysis between the IP2 and Input2 samples (Fig. 3B). The two replicates of experimental data showed uneven data quality. Since the peak of IP2 had more obvious enrichment near the transcription initiation site (Fig. 3C), the data of IP2 were selected for subsequent integration analysis. The ChIP-seq data of MAPK1 in AGS cells were then systematically analyzed.

A total of 92,898 peaks and 6,493 peak-associated genes were discovered using the IP2 data of ChIP-seq. After

identification, we found that all these binding peaks contained one or more MAPK1 binding motifs. Through this analysis, we identified binding motifs shared by several peaks and display the 10 most drastically enhanced binding motifs (Fig. 3E) (full list in Table S6). In particular, we enriched the binding motif of G/CAAAG/C in both IP1 and IP2 samples, which was consistent with the previously reported binding motif of MAPK1 in Hela cells [19].

Through GO annotation and KEGG pathway enrichment, MAPK1 target genes were shown to be concentrated in the biological processes of defence, signal transduction, the G protein-coupled receptor signalling pathway, and the circadian control of gene expression (Fig. 3F). The NOD-like receptor signalling route, the Hippo signalling pathway, and the TGF-beta signalling
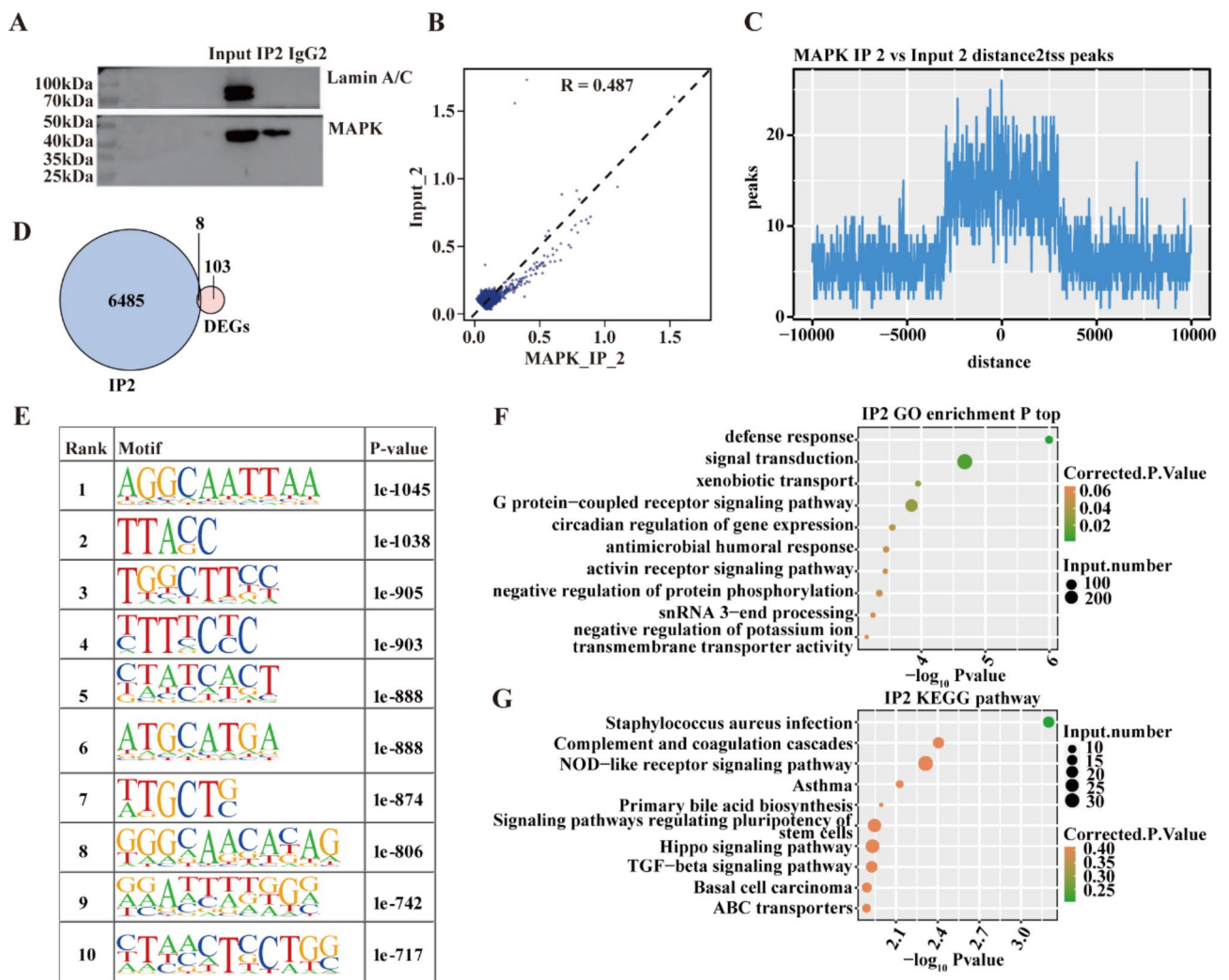

Fig. 3 MAPK1 extensively interacts with genes by binding to their promoter region. (**A**) The Western blot result plot for MAPK1 ChIP. (**B**) Sample correlation. (**C**) ChIP-seq enrichment around TSS regions in IP2. (**D**) Venn diagram depicting overlapping genes between MAPK1 target genes and DEGs. (**E**) Motif analysis results show the enriched motifs from MAPK1 target peaks from the IP2. (**F**) A bubble plot of the top 10 enriched GO bp terms for the genes that are coupled to MAPK1. (**G**) The top 10 enriched KEGG pathways of MAPK1 target genes are shown in a bubble plot

Wang *et al. BMC Cancer*   (2023) 23:959

Page 9 of 13

pathway were among the enriched KEGG pathways (Fig. 3G).

Identification of MAPK1 target genes in AGS cells

By integrating the RNA-seq and ChIP-seq results, overlapping analysis of MAPK1 target genes in IP2 data with DEGs after *MAPK1* knockdown obtained a total of eight target genes, whose DNA regulatory regions were bound by MAPK1 and expressions were meanwhile markedly associated with the knockdown of MAPK1 (Fig. 3D), i.e., *FGG*, *KRT6A*, *KRT13*, *KRT81*, *MYH15*, *STARD4*, *SYTL4*, and *TMEM267*. It was worth noting that MAPK1 demonstrated bidirectional regulatory functions on these genes, repressing the expression of *FGC* whilst activating the expressions of the other seven (*KRT6A*, *KRT13*, *KRT81*, *MYH15*, *STARD4*, *SYTL4*, and *TMEM267*) in AGS cells.

Among them, three genes, i.e., *KRT6A*, *KRT13*, and *KRT81*, were related to cancer metastasis and migration. We next used an integrative genomics viewer (IGV) [39] to visualise the peak reads and binding locations throughout the mRNA by Sashimi Plot for these three genes (Fig. 4A). Our results indicated that MAPK1 may activate these three target genes (*KRT81*, *KRT6A*, and *KRT13)* by binding to their promotor regions.

Additionally, survival analysis was conducted in the TCGA gastric cancer database to further assess the clinical importance of these eight target genes in gastric cancer. Kaplan-Meier survival analysis of two subgroups based on the expressions of six genes (*FGG*, *KRT6A*, *KRT13*, *KRT81*, *MYH15*, and *TMEM267*) predicted distinct survial outcomes (Fig. 4B, Fig S1, S2 and S3). Patient outcomes were not significantly influenced by expressions of *STARD4* and *SYTL4* (Fig S4 and S5).

Discussion

Several types of cancer have been shown to have aberrant MAPK1 expression, mounting evidence that MAPK1 is linked to cancer invasion and metastasis [40–42]. In prostate cancer cells, for instance, TGF-β therapy leads to nuclear accumulation of MAPK1, which in turn promotes cancer cell EMT and upregulates the production of MMP1, MMP2/9, and MMP9 [43]. To facilitate cancer cell migration and decrease adhesion, transcription factor Snail in breast cancer may stimulate nuclear translocation of phosphorylated MAPK [44]. The involvement of MAPK in mediating extracellular matrix activity may alter gastric cancer cell invasion and migration. The MAPK/ERK pathways have been shown to play a role in controlling gastric cancer cell migration and invasion induced by IL-22, PRL3, NAIF1, and CCDC134 [45]. Inhibiting gastric cancer growth by competitive binding to MEK1, as the MAPK1-109aa expressed by *circMAPK1*, is one of the mechanisms by which it works to deactivate

MAPK1 and its downstream components in the MAPK pathway [46]. However, previous research has concentrated on MAPK1 as a kinase that controls cancer's ability to invade and spread. Its function as a transcription regulator by DNA binding activity in cancer cells and the role it plays in the invasion and spread of cancer are mostly unknown.

One of the hallmarks of cancer is its tendency to metastasize [9]. Tumour cell invasiveness, epithelial-mesenchymal transition features, tumour cell-cancer microenvironment communication, and extracellular matrix remodelling all play a role in tumour metastasis [47–49]. Metastasis is therefore a leading cause of mortality for people with gastric cancer. MAPK1 is an essential oncogene that stimulates gastric cancer's cell proliferation, migration, and invasion and an increased level of MAPK1 expression is associated with a higher risk of developing gastric cancer [50]. Our study shows that AGS cell invasion and migration are dramatically facilitated by MAPK1 overexpression. As a result, we postulated that MAPK1 promotes gastric cancer cell metastasis and invasion through its gene-binding function, ability to combine the promoter area of target genes, effects on the target genes expression, and effects on protein level.

Against the above backdrop, we used *MAPK1* knockdown in AGS cells and RNA-seq to test this theory. Our study identified the risk and protective gene sets for the migration and invasion of AGS cells. Of a total of 111 DEGs, 80 of them were significantly downregulated and 31 were upregulated. GO enrichment analysis reveals that the majority of downregulated genes are involved in activities including promoting gene expression, preventing apoptosis, and positively regulating cell proliferation. Ten typical genes involved in cellular metastasis are among the genes that were repressed here (Fig. 2F). Thus, MAPK1 shows the ability to increase AGS cell invasion and migration by activating these risk genes.

Next, we used ChIP-seq to investigate the MAPK1 binding genes at a genome-wide scale. We found that 6,493 genes had 92,898 binding peaks. Together, the findings from the ChIP-seq and RNA-seq analyses revealed eight genes whose expression is controlled by MAPK1 and whose binding to MAPK1 was previously unknown. *KRT81*, *KRT6A*, and *KRT13* are examples of these genes that have been linked to cancer metastasis and migration in humans [51–55]. In summary, ChIP-seq combined with RNA-seq revealed that MAPK1 selectively binds to the promoter regions of *KRT81*, *KRT6A*, and *KRT13* genes and regulates their transcription. This function of MAPK1 in regulating gene expression may be related to cancer invasion and metastasis. These results provide credence to the idea that MAPK1 promotes cancer cell invasion and migration via binding to the promoter regions of *KRT81*, *KRT6A*, and *KRT13*.
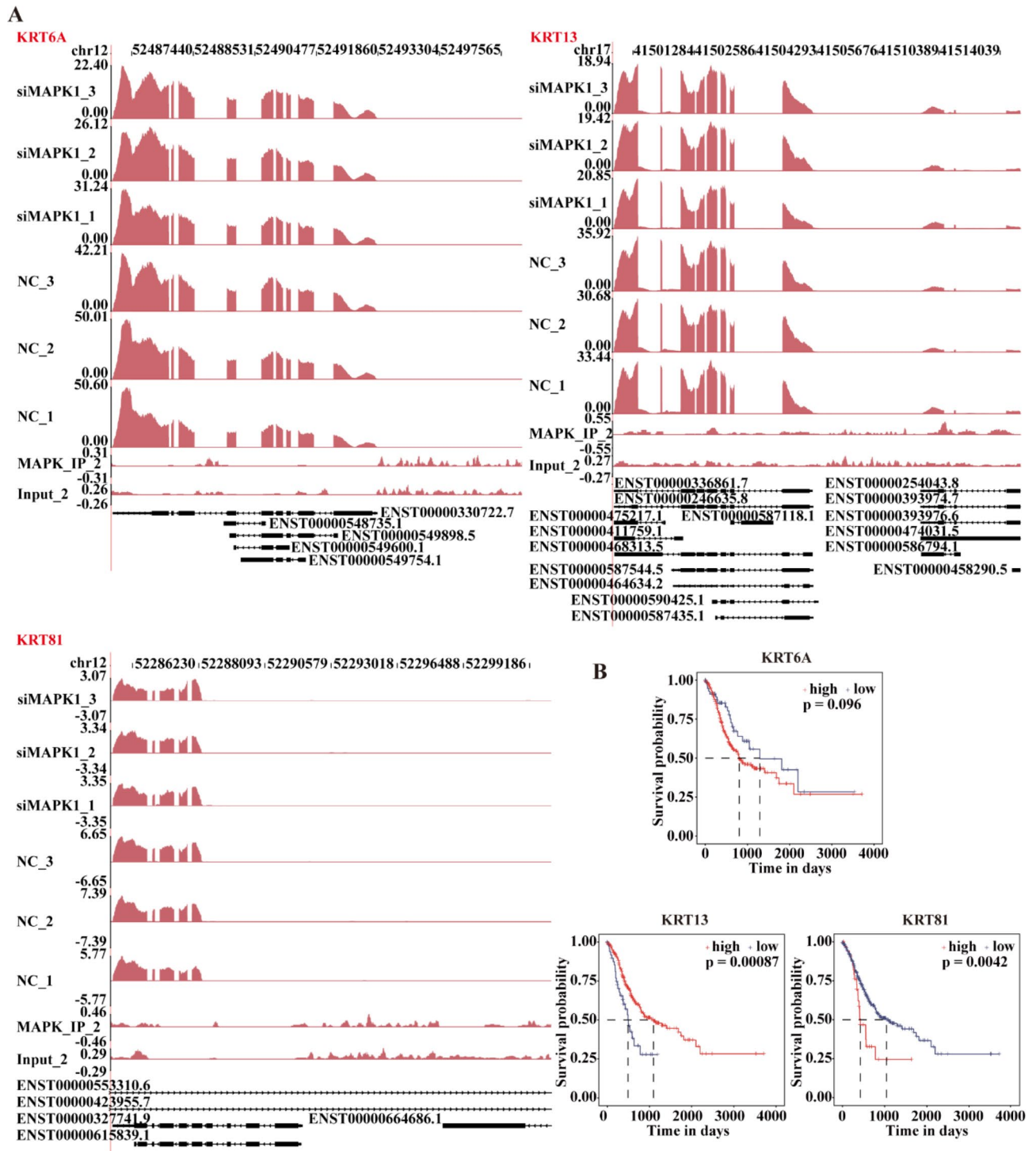
Fig. 4 Validation of interacting genes associated with MAPK1. (**A**) The peak reads and binding locations throughout the mRNA are shown in the IGV Sashimi Plot. The red sections indicate the peak positions. The transcripts for each gene are shown below, and the read distribution of the bound gene is plotted in the top panel. (**B**) Prognostic line plots of a few significant genes from the TCGA data on gastric cancer. siMAPK1: short interfering MAPK1; NC: non-targeting control; Input: background noise without undergoing immunoprecipitation

Over 1800 TFs are being identified in the human genome [21]. MAPK1 showed its role as a transcription repressor besides protein kinases in a previous study using experiments in Hela cells, and the DNA binding motif of MAPK1 in this cell model was identified as G/CAAAG/C [19]. The present study validates this DNA binding motif of MAPK1 in AGS cells, by which MAPK1 represses the target gene (*FGC*) (Fig. 3E). Furthermore, our study contributes a list of novel DNA binding motifs for MAPK1 in gastric cancer and demonstrates that MAPK1 can function as a bidirectional transcription factor that activates and represses the transcriptions of different target genes in gastric cancer cells. This finding supports the emerging views that many TFs have opposite regulatory effects on different genes relying on differentiating local binding motifs and recruiting multiple cofactors available in different environments [56, 57]. Identifying the tissue-specific and cell-specific functions of transcription factors and understanding their functions is important for understanding the comprehensive molecular regulations underlying cell proliferation and cancer progression [58, 59]. The new mechanism of MAPK1 as a bidirectional transcription factor provides a theoretical basis for the development of combined drugs to inhibit MAPK1 activity from multiple perspectives, offering a promising avenue for targeted GC treatment. Additionally, the identification of target genes regulated by MAPK1 in this study unveils novel candidate molecules with potential therapeutic implications for GC.

Recent developments in experimental technologies, including RNA-seq and ChIP-seq, are revolutionized appoaches for identifying DNA binding sites for a TF of interest [60, 61]. However, several limitations in the present study need to be discussed. First, ChIP-seq provides information on the genomic regions that are bound by a specific protein, but the resolution of the technique is limited by the size of the DNA fragments that are generated during the experiment. This can make it difficult to precisely locate binding sites within larger genomic regions. Secondly, the technical variability can influence the mapping results of TF binding sites, for example, differences in the quality of the antibodies used for immunoprecipitation, variations in sample preparation, and differences in sequencing depth. Being focused on a single-cell line, the current study may limit its potential impacton on the generalisability and applicability of our findinds to other GC cell lines or tissues. Conducting further research involving a variety of GC cell lines and tissues are needed in the future to enhance the broader relevance of current results. In addition, restrictions in the efficiency of the immunoprecipitation step, or the fact that some regions may be inaccessible in terms of chromatin structure can lead to incomplete coverage for binding sites investigation. Last but not the least, ChIP-seq provides information on the genomic regions that are bound by a specific protein, but it does not provide information on the protein-protein interactions that may be involved in regulating gene expression. The limited information on protein-protein interactions, especially on the factors collaborating with a master transcription regulator, appeals to more systematic studies.

Conclusions

In conclusion, our findings show that MAPK1 knockdown significantly increases invasiveness and migration in gastric cancer cells. MAPK1 can function in gastric cancer metastasis and invasion as a bidirectional transcription factor. Furthermore, elevated levels of MAPK1 target genes in gastric cancer patients can be bound to the promoter regions to increase or decrease their expression, thereby facilitating gastric cell migration and invasion.

Abbreviations

AGS cells	A human gastric adenocarcinoma cell-line
CA	California
CCDC134	Coiled-coil domain containing 134
CCND1	Cyclin D1
CDS	coding sequence
ChIP	Chromatin immunoprecipitation
CXCL8	C-X-C motif chemokine ligand 8
DEG	Differentially expressed gene
DNA	Deoxyribonucleic acid
EDTA	Ethylenediaminetetraacetic acid
EMP3	Epithelial membrane protein 3
ERK2	Eextracellular signal-regulated kinases 2
FDR	False discovery rate
FGG	Fibrinogen gamma chain
FPKM	Fragments per kilobase million
GAPDH	Glyceraldehyde-3-phosphate dehydrogenase
GO	Gene Ontology
IL-22	Interleukin 22
ITGA2	Integrin subunit alpha 2
KEGG	Kyoto Encyclopedia of Genes and Genomes
KOBAS	KEGG Orthology-Based Annotation System
KRT	Keratin
MA	Massachusetts
MAL2	Mal, T cell differentiation protein 2
MAPK1	Mitogen-activated protein kinase 1
MD	Maryland
MEK	Meiotic chromosome-axis-associated kinase
MYH15	Myosin heavy chain 15
NAIF1	Nuclear apoptosis inducing factor 1
NOD	Nucleotide binding oligomerization domain
PAD	Peptidylarginine deiminase
PCA	Principal component analysis
PRL3	Protein-tyrosine phosphatase of regenerating liver 3
qRT-PCR	Quantitative reverse transcription polymerase chain reaction
SDS-PAGE	Sodium dodecyl sulphate polyacrylamide gel electrophoresis
SEM	Standard error of the mean
siRNAs	Short interfering ribonucleic acid
STARD4	Steroidogenic acute regulatory protein-related lipid transfer domain containing 4
SYTL4	Synaptotagmin like 4
TGF-beta	Transforming growth factor beta
TMEM267	Transmembrane protein 267
TSS	Transcription start site
USA	United States of America
WI	Wisconsin

Wang *et al. BMC Cancer*   (2023) 23:959

Page 12 of 13

Supplementary Information

The online version contains supplementary material available at https://doi.org/10.1186/s12885-023-11480-3.

Supplementary Material 1

Supplementary Material 2

Authors' contributions
Yue Wang, Xingang Li and Ying Song designed the experiments; Yue Wang, Zheng Guo, Yueli Tian, Liang Cong, Yulu Zheng and Guangle Shan conducted most experiments; Yue Wang, Zhiyuan Wu, and Ying Song analyzed the experimental data; Yahong Zhu, Yao Xia and Xingang li performed bioinformatic analyses; Yue Wang, Zheng Guo, Xingang Li, and Ying Song wrote, reviewed, and revised the manuscript; Xingang Li and Ying Song conceived the project, supervised the study, provided overall guidance, and finalized the manuscript. All authors read and approved the final manuscript.

Data Availability
The RNA-seq and ChIP-seq datasets generated in this study are available at the Gene Expression Ominbus (GEO, https://www.ncbi.nlm.nih.gov/geo/) repository accession number GSE234020 and GSE234022. The gene expression and clinical data of gastric cancer are publicly available in the TCGA database (https://portal.gdc.cancer.gov). Other datasets used and/or analyzed during the current study will be made available upon reasonable request from the corresponding authors.

Declarations

Competing interests
The authors declare that they have no conflict of interest.

Ethics approval and consent to participate
The human gastric adenocarcinoma epithelial cell line (AGS cells, CRL-1739) utilized in this research was obtained from American Type Culture Collection (ATCC, Rockville, MD, USA), which is a commercially available cell line, and therefore, informed consent from patients is not applicable in this context and patient identifier and personal information have been removed from this product. Our study has been conducted in accordance with the ethical guidelines and regulations set forth by our institution.

Consent for publication
Not applicable.

References
1. Smyth EC, Nilsson M, Grabsch HI, van Grieken NC, Lordick F. Gastric cancer. Lancet. 2020;396(10251):635–48.
2. Machlowska J, Baj J, Sitarz M, Maciejewski R, Sitarz R. Gastric Cancer: epidemiology, risk factors, classification, genomic characteristics and treatment strategies. Int J Mol Sci 2020, 21(11).
3. Bray F, Ferlay J, Soerjomataram I, Siegel RL, Torre LA, Jemal A. Global cancer statistics 2018: GLOBOCAN estimates of incidence and mortality worldwide for 36 cancers in 185 countries. CA Cancer J Clin. 2018;68(6):394–424.
4. Nakamura K, Sugano H, Takagi K. Carcinoma of the stomach in incipient phase: its histogenesis and histological appearances. Gan. 1968;59(3):251–8.
5. Lauren P, THE TWO HISTOLOGICAL MAIN TYPES OF GASTRIC CARCINOMA: DIFFUSE AND SO-CALLED INTESTINAL-TYPE CARCINOMA. AN ATTEMPT AT A HISTO-CLINICAL CLASSIFICATION. Acta Pathol Microbiol Scand. 1965;64:31–49.
6. Kushima R. The updated WHO classification of digestive system tumours-gastric adenocarcinoma and dysplasia. Pathologe. 2022;43(1):8–15.
7. Digklia A, Wagner AD. Advanced gastric cancer: current treatment landscape and future perspectives. World J Gastroenterol. 2016;22(8):2403–14.
8. Fock KM. Review article: the epidemiology and prevention of gastric cancer. Aliment Pharmacol Ther. 2014;40(3):250–60.
9. Arnold M, Abnet CC, Neale RE, Vignat J, Giovannucci EL, McGlynn KA, Bray F. Global burden of 5 major types of gastrointestinal cancer. Gastroenterology. 2020;159(1):335–349e315.
10. Joshi SS, Badgwell BD. Current treatment and recent progress in gastric cancer. CA: Cancer J Clin. 2021;71(3):264–79.
11. Sturgill TW, Ray LB, Erikson E, Maller JL. Insulin-stimulated MAP-2 kinase phosphorylates and activates ribosomal protein S6 kinase II. Nature. 1988;334(6184):715–8.
12. Boulton TG, Nye SH, Robbins DJ, Ip NY, Radziejewska E, Morgenbesser SD, DePinho RA, Panayotatos N, Cobb MH, Yancopoulos GD. ERKs: a family of protein-serine/threonine kinases that are activated and tyrosine phosphorylated in response to insulin and NGF. Cell. 1991;65(4):663–75.
13. Vomastek T, Iwanicki MP, Burack WR, Tiwari D, Kumar D, Parsons JT, Weber MJ, Nandicoori VK. Extracellular signal-regulated kinase 2 (ERK2) phosphorylation sites and docking domain on the nuclear pore complex protein tpr cooperatively regulate ERK2-Tpr interaction. Mol Cell Biol. 2008;28(22):6954–66.
14. Dong C, Davis RJ, Flavell RA. MAP kinases in the immune response. Annu Rev Immunol. 2002;20:55–72.
15. Wang Y, Li M, Zeng J, Yang Y, Li Z, Hu S, Yang F, Wang N, Wang W, Tie J. MiR-585-5p impedes gastric cancer proliferation and metastasis by orchestrating the interactions among CREB1, MAPK1 and MITF. Front Immunol. 2022;13:1008195.
16. AACR Project GENIE Consortium. AACR Project GENIE: powering precision medicine through an international consortium. Cancer Discov. 2017;7(8):818–31.
17. Hu L, Wu H, Wan X, Liu L, He Y, Zhu L, Liu S, Yao H, Zhu Z. MicroRNA-585 suppresses tumor proliferation and migration in gastric cancer by directly targeting MAPK1. Biochem Biophys Res Commun. 2018;499(1):52–8.
18. Fei B, Wu H. MiR-378 inhibits progression of human gastric cancer MGC-803 cells by targeting MAPK1 in vitro. Oncol Res. 2012;20(12):557–64.
19. Hu S, Xie Z, Onishi A, Yu X, Jiang L, Lin J, Rho HS, Woodard C, Wang H, Jeong JS, et al. Profiling the human protein-DNA interactome reveals ERK2 as a transcriptional repressor of interferon signaling. Cell. 2009;139(3):610–22.
20. Spitz F, Furlong EE. Transcription factors: from enhancer binding to developmental control. Nat Rev Genet. 2012;13(9):613–26.
21. Lambert SA, Jolma A, Campitelli LF, Das PK, Yin Y, Albu M, Chen X, Taipale J, Hughes TR, Weirauch MT. The human transcription factors. Cell. 2018;172(4):650–65.
22. Bushweller JH. Targeting transcription factors in cancer - from undruggable to reality. Nat Rev Cancer. 2019;19(11):611–24.
23. Park M, Kang KW, Kim JW. The role and application of transcriptional repressors in cancer treatment. Arch Pharm Res. 2023;46(1):1–17.
24. Kozera B, Rapacz M. Reference genes in real-time PCR. J Appl Genet. 2013;54(4):391–406.
25. Livak KJ, Schmittgen TD. Analysis of relative gene expression data using real-time quantitative PCR and the 2(-Delta Delta C(T)) method. Methods. 2001;25(4):402–8.
26. Yuan B, Latek R, Hossbach M, Tuschl T, Lewitter F. siRNA selection server: an automated siRNA oligonucleotide prediction server. Nucleic Acids Res 2004, 32(Web Server issue):W130–134.
27. Langmead B, Salzberg SL. Fast gapped-read alignment with Bowtie 2. Nat Methods. 2012;9(4):357–9.
28. Trapnell C, Williams BA, Pertea G, Mortazavi A, Kwan G, van Baren MJ, Salzberg SL, Wold BJ, Pachter L. Transcript assembly and quantification by RNA-Seq reveals unannotated transcripts and isoform switching during cell differentiation. Nat Biotechnol. 2010;28(5):511–5.

29. Robinson MD, McCarthy DJ, Smyth GK. edgeR: a Bioconductor package for differential expression analysis of digital gene expression data. Bioinformatics. 2010;26(1):139–40.

30. Zhang Y, Liu T, Meyer CA, Eeckhoute J, Johnson DS, Bernstein BE, Nusbaum C, Myers RM, Brown M, Li W, et al. Model-based analysis of ChIP-Seq (MACS). Genome Biol. 2008;9(9):R137.

31. Kidder BL, Hu G, Zhao K. ChIP-Seq: technical considerations for obtaining high-quality data. Nat Immunol. 2011;12(10):918–22.

32. Ramírez F, Ryan DP, Grüning B, Bhardwaj V, Kilpert F, Richter AS, Heyne S, Dündar F, Manke T. deepTools2: a next generation web server for deep-sequencing data analysis. Nucleic Acids Res. 2016;44(W1):W160–165.

33. Heinz S, Benner C, Spann N, Bertolino E, Lin YC, Laslo P, Cheng JX, Murre C, Singh H, Glass CK. Simple combinations of lineage-determining transcription factors prime cis-regulatory elements required for macrophage and B cell identities. Mol Cell. 2010;38(4):576–89.

34. Robinson JT, Thorvaldsdóttir H, Winckler W, Guttman M, Lander ES, Getz G, Mesirov JP. Integrative genomics viewer. Nat Biotechnol. 2011;29(1):24–6.

35. Xie C, Mao X, Huang J, Ding Y, Wu J, Dong S, Kong L, Gao G, Li CY, Wei L. KOBAS 2.0: a web server for annotation and identification of enriched pathways and diseases. Nucleic Acids Res 2011, 39(Web Server issue):W316–322.

36. Kanehisa M, Furumichi M, Sato Y, Kawashima M, Ishiguro-Watanabe M. KEGG for taxonomy-based analysis of pathways and genomes. Nucleic Acids Res. 2023;51(D1):D587–d592.

37. Liu J, Lichtenberg T, Hoadley KA, Poisson LM, Lazar AJ, Cherniack AD, Kovatich AJ, Benz CC, Levine DA, Lee AV, et al. An integrated TCGA pan-cancer clinical data resource to drive high-quality survival outcome analytics. Cell. 2018;173(2):400–416e411.

38. Andrews S. FastQC: a quality control tool for high throughput sequence data [Online]. In.; 2010.

39. Robinson JT, Thorvaldsdóttir H, Wenger AM, Zehir A, Mesirov JP. Variant review with the Integrative Genomics Viewer. Cancer Res. 2017;77(21):e31–34.

40. Zhu L, Yang S, Wang J. miR-217 inhibits the migration and invasion of HeLa cells through modulating MAPK1. Int J Mol Med. 2019;44(5):1824–32.

41. Gagliardi M, Pitner MK, Park J, Xie X, Saso H, Larson RA, Sammons RM, Chen H, Wei C, Masuda H, et al. Differential functions of ERK1 and ERK2 in lung metastasis processes in triple-negative breast cancer. Sci Rep. 2020;10(1):8537.

42. Yu TT, Wang CY, Tong R. ERBB2 gene expression silencing involved in ovarian cancer cell migration and invasion through mediating MAPK1/MAPK3 signaling pathway. Eur Rev Med Pharmacol Sci. 2020;24(10):5267–80.

43. Amatangelo MD, Goodyear S, Varma D, Stearns ME. c-Myc expression and MEK1-induced Erk2 nuclear localization are required for TGF-beta induced epithelial-mesenchymal transition and invasion in prostate cancer. Carcinogenesis. 2012;33(10):1965–75.

44. Smith BN, Burton LJ, Henderson V, Randle DD, Morton DJ, Smith BA, Taliaferro-Smith L, Nagappan P, Yates C, Zayzafoon M, et al. Snail promotes epithelial mesenchymal transition in breast cancer cells in part via activation of nuclear ERK2. PLoS ONE. 2014;9(8):e104987.

45. Yang M, Huang CZ. Mitogen-activated protein kinase signaling pathway and invasion and metastasis of gastric cancer. World J Gastroenterol. 2015;21(41):11673–9.

46. Jiang T, Xia Y, Lv J, Li B, Li Y, Wang S, Xuan Z, Xie L, Qiu S, He Z, et al. A novel protein encoded by circMAPK1 inhibits progression of gastric cancer by suppressing activation of MAPK signaling. Mol Cancer. 2021;20(1):66.

47. Fares J, Fares MY, Khachfe HH, Salhab HA, Fares Y. Molecular principles of metastasis: a hallmark of cancer revisited. Signal Transduct Target Ther. 2020;5(1):28.

48. Liu Q, Zhang H, Jiang X, Qian C, Liu Z, Luo D. Factors involved in cancer metastasis: a better understanding to seed and soil hypothesis. Mol Cancer. 2017;16(1):176.

49. Huang Q, Liu M, Zhang D, Lin BB, Fu X, Zhang Z, Zhang B, Dong JT. Nitazoxanide inhibits acetylated KLF5-induced bone metastasis by modulating KLF5 function in prostate cancer. BMC Med. 2023;21(1):68.

50. Luo M, Liang C. LncRNA LINC00483 promotes gastric cancer development through regulating MAPK1 expression by sponging miR-490-3p. Biol Res. 2020;53(1):14.

51. Nanashima N, Horie K, Yamada T, Shimizu T, Tsuchida S. Hair keratin KRT81 is expressed in normal and breast cancer cells and contributes to their invasiveness. Oncol Rep. 2017;37(5):2964–70.

52. Yang B, Zhang W, Zhang M, Wang X, Peng S, Zhang R. KRT6A promotes EMT and cancer stem cell transformation in lung adenocarcinoma. Technol Cancer Res Treat. 2020;19:1533033820921248.

53. Yin L, Li Q, Mrdenovic S, Chu GC, Wu BJ, Bu H, Duan P, Kim J, You S, Lewis MS, et al. KRT13 promotes stemness and drives metastasis in breast cancer through a plakoglobin/c-Myc signaling pathway. Breast Cancer Res. 2022;24(1):7.

54. Che D, Wang M, Sun J, Li B, Xu T, Lu Y, Pan H, Lu Z, Gu X. KRT6A promotes lung cancer cell growth and invasion through MYC-regulated pentose phosphate pathway. Front Cell Dev Biol. 2021;9:694071.

55. Zhang K, Liang Y, Zhang W, Zeng N, Tang S, Tian R. KRT81 knockdown inhibits malignant progression of melanoma through regulating interleukin-8. DNA Cell Biol. 2021;40(10):1290–7.

56. Wong KH, Struhl K. The Cyc8-Tup1 complex inhibits transcription primarily by masking the activation domain of the recruiting protein. Genes Dev. 2011;25(23):2525–39.

57. Schmitges FW, Radovani E, Najafabadi HS, Barazandeh M, Campitelli LF, Yin Y, Jolma A, Zhong G, Guo H, Kanagalingam T, et al. Multiparameter functional diversity of human C2H2 zinc finger proteins. Genome Res. 2016;26(12):1742–52.

58. Li X, Wang H, Zhu Y, Cao W, Song M, Wang Y, Hou H, Lang M, Guo X, Tan X, et al. Heritability enrichment of immunoglobulin G N-glycosylation in specific tissues. Front Immunol. 2021;12:741705.

59. Li X, Wang L, Tan X, Wang W. Chap. 13 - Genome plasticity and endocrine diseases. In: Forero DA, Patrinos GP, editors. Genome plasticity in health and disease. Academic Press; 2020. p. 211–235.

60. Stark R, Grzelak M, Hadfield J. RNA sequencing: the teenage years. Nat Rev Genet. 2019;20(11):631–56.

61. Park PJ. ChIP-seq: advantages and challenges of a maturing technology. Nat Rev Genet. 2009;10(10):669–80.

Publisher's Note